Chapter 8
Structural Health Monitoring Performance During the 2010 Gigantic Chile Earthquake

Rubén Luis Boroschek

Abstract In February 27, 2010, the sixth largest magnitude earthquake recoded in the world affected the central part of Chile. More than 1,500 buildings higher than ten stories, bridges, and dams suffered strong shaking. Only three buildings and one bridge in all the stock were instrumented, a clear deficiency for such an active seismic area of the world. Review of the damage to the buildings' stock took more than 1 month with a high social and political pressure to give assurance on the level of damage of each building. One of the instrumented buildings had a continuous remote monitoring system, and it gave in less than 10 min after the earthquake, an indication of the level of change in dynamic properties. For the other two buildings, the earthquake data was retrieved, and a detailed visual and analytical description of the observed damage and change of the modal properties was given in less than a week, due to an already existing algorithm of system identification and response parameter characterizations. These examples indicate the important potential of structural heal monitoring for rapid response and damage assessment of structures.

Keywords Real-Time Monitoring • Earthquake damage • System Identification • Chile • SHM • Structural Health Monitoring

8.1 The Earthquake

The Mw 8.8 Chile earthquake occurred on February 27, 2010, in the south central Chilean region of Maule. This earthquake is associated with the subduction process of the Nazca plate beneath the South American plate, and it is one of the largest magnitude events to have produced strong motion recordings worldwide. Finite

R.L. Boroschek (✉)
Civil Engineering Department, University of Chile, Blanco Encalada 2002 Piso 4, Santiago, Chile
e-mail: rborosch@ing.uchile.cl

M. Garevski (ed.), *Earthquakes and Health Monitoring of Civil Structures*,
Springer Environmental Science and Engineering, DOI 10.1007/978-94-007-5182-8_8,

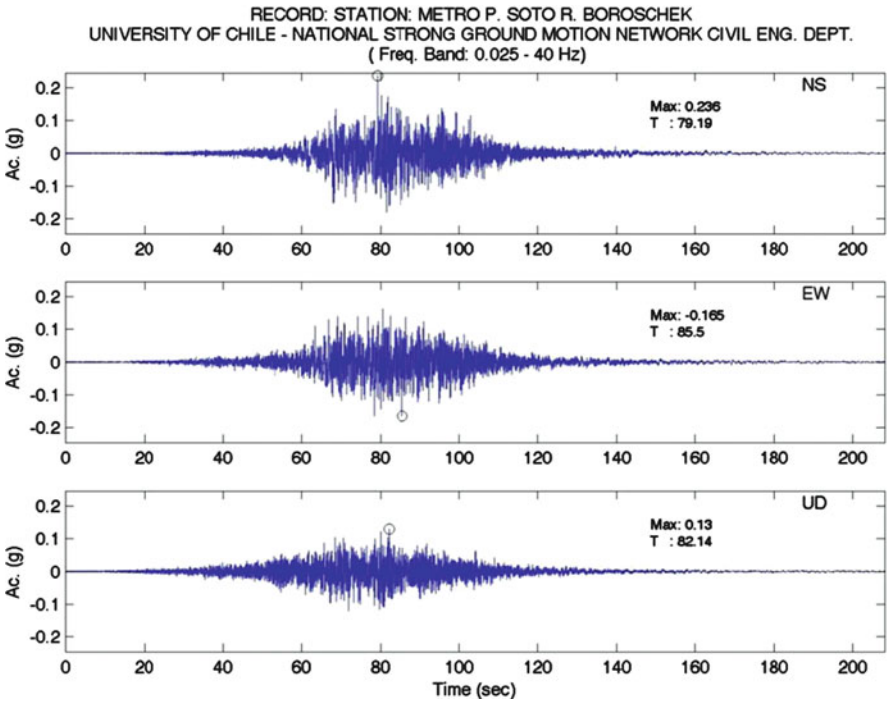

Fig. 8.1 Representative free field station in Santiago. Metro Mirador record

fault models of the earthquake rupture have been generated by several authors; Delouis et al. (2010) indicated a rupture fault plane to envelope the high-slip region with a dimension of 530 by 150 km.

Only 36 strong motion records are publically available from this earthquake. It is not expected that the total amount of acceleration records of the main event to be much larger. Detailed analysis of records is presented by Boroschek et al. (2012), so they are not present here. The maximum PGA was 0.93 g at station at Angol city located in the extreme south of the rupture area, and the maximum peak ground velocity was 67 cm/s at the constitución at the center of the rupture. Significant durations according to 5–95% of Arias intensity ranged from about 30–90 s, although perceptible durations were often much longer at 2–3 min.

The instrumented buildings are located in the capital city of Chile Santiago. In Santiago, most of the tall buildings are located in predominant stiff soils. Nevertheless, areas on the northern or eastern part of the city present intermediate soils (Assimaki et al. 2012). Representative records of the motions in Santiago are Hospital Sotero del Rio (HSOR), Hospital Tisne (HTIS), Santa Lucia (SLUC), Antumapu (ANTU), Maipu (CRMA), Andalucia (SANT), and Metro Mirador (MET). The characteristic record of Metro Mirador is presented in Fig. 8.1, and

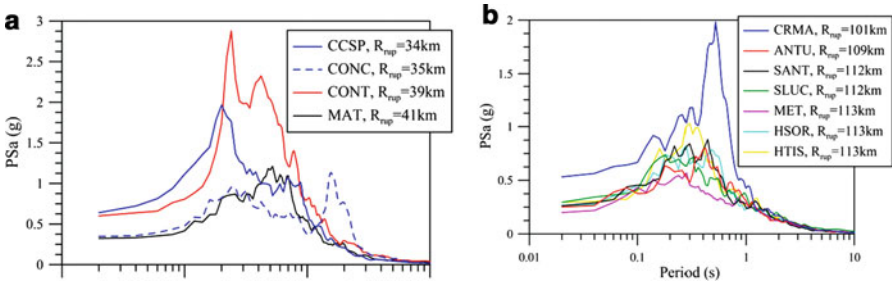

Fig. 8.2 Representative response spectra

the geometric mean spectra of the horizontal components of the critical Santiago records in Fig. 8.2.

As can be seen from Fig. 8.1, the record has a rather slow start due to the 110-km distance to the fault rupture and the extent of the rupture area. Horizontal envelopes of accelerations are rather smooth with shaking larger than 0.1 g for more than 30 s. In the vertical direction, acceleration is larger than 0.05 g for more than 40 s. This large amplitudes and duration contributed to damage and panic that affected the population in the highest hit areas.

The closest instruments to the fault plane are in Concepción city: CCSP (relatively firm soil) and CONC (relatively soft soil) with rupture distances of 34–35 km. In Fig. 8.2, we present the geometric mean 5% damping response spectra of these records. The relatively firm soil conditions at CCSP produced large spectral peaks above 2 g at short periods (~0.2 s), while the softer conditions at CONC produced much lower short period spectral accelerations and a pronounced spectral peak from 1.5 to 2.2 s. The Constitución station (CONT soft soil) has much higher spectral ordinates over a broad period range (0.2–1.5 s), which can be associated with a site effect that is much more broadly banded than that at CONC.

Santiago response spectra with the exception of CRMA station present maximum demands between 0.2 and 0.6 s; this is typical of the stiff gravelly soils of the area. In these cases, the maximum spectral demands are close to 1 g in the indicated period range.

8.2 University of Chile Torre Central Building

One of the instrumented buildings, called Torre Central, was constructed in 1962. It is located at the Engineering Faculty of the University of Chile. The building has office and classroom use. It has nine stories above ground, two underground levels, and a total surface area of 4,602 m^2. It has a total height of 30.2 m and a plan area of 30 m $\times$ 19 m (Fig. 8.3). The structural system consists of reinforced concrete shear

Fig. 8.3 Torre Central general view

walls. Typical wall thickness is 35 cm and typical slab thickness is 25 cm. The ratio between total wall area and plan area for all above ground stories is 7.7%.

The building has been studied using ambient vibration since its construction in the early 1960, but no permanent instrumentation was located in the building until 2009 where a permanent remote structural health monitoring system was installed in the building (Boroschek et al. 2010).

8.2.1 Instrumentation and Sensor Layout

The building was instrumented as part of the structural health monitoring research activities of the University of Chile with the support of Chilean Council of Science and Technology. The objective of the research and instrumentation is to continuously monitor the response and the modal parameters of the structural system in order to evaluate, as example, modeling criteria for wall buildings, effect of ambient and soil conditions on the modal parameters of the structure, software development for concurrent ambient and seismic vibrations, development of seismic alert system based on response and modal parameters of the structure, effect of amplitude response on the modal parameters, and damage detection algorithms.

8.2.1.1 Sensor Location

The system has eight force balance accelerometers, configured in a range +/− 1 [g] with two parallel acquisition systems: the first one, the seismic records with a trigger configuration; the second, with an amplification of the analog signal to capture continuously the ambient vibrations. The accelerometer location is shown in Fig. 8.4. Three sensors are located horizontally on the third and eighth floors, and two sensors are at the foundation level. This sensor distribution allows for the monitoring of the spatial motion of the structure, the identification of the modal

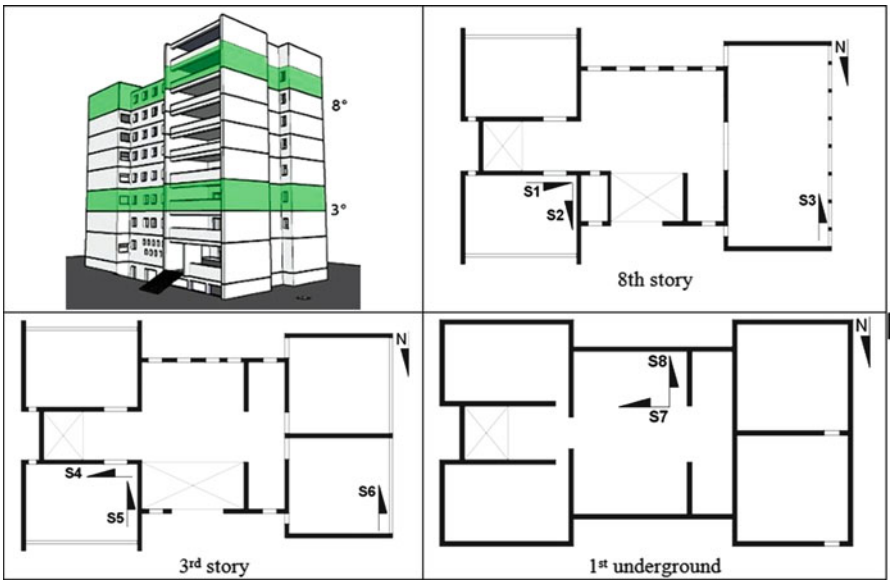

Fig. 8.4 Accelerometer location

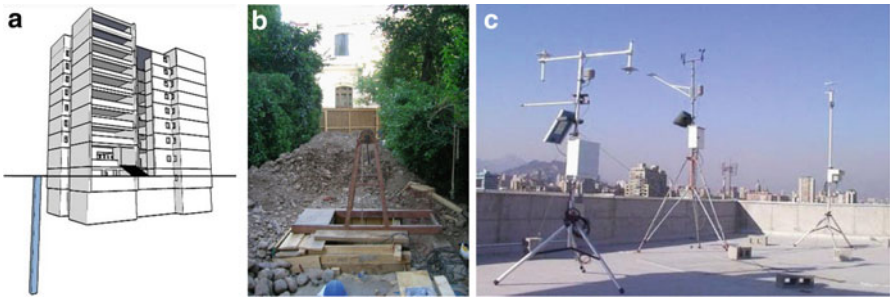

Fig. 8.5 Sensors: (**a**) schematic dwell location, (**b**) well for humidity sensors, and (**c**) meteorological station

properties, and the partial capturing of its linear and nonlinear response characteristics.

The sensors register the analog acceleration with a dynamic range of 135 dB between 0.01 and 50 Hz and 145 dB between 0.01 and 20 Hz. The analog signal is converted into a digital record in a central recording unit with a 16-bit resolution. Sampling rate for these sensors is 100 Hz. These sensors are used to identify the structural properties and response parameters.

Additionally, three humidity sensors have been installed in a well in the west side of the building. The humidity sensors are located at 20, 10, and 5 m below the surface, and they are connected to the accelerometer data acquisition system,

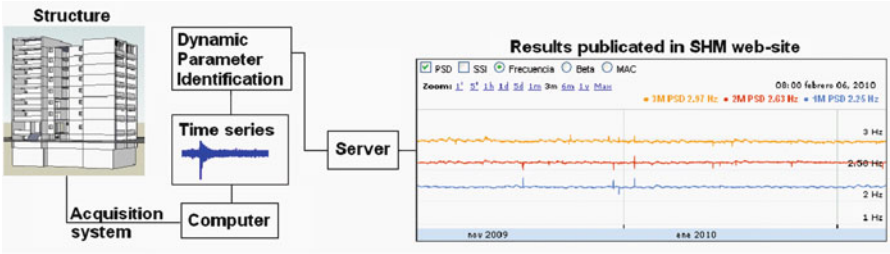

Fig. 8.6 Structural health monitoring network workflow

Fig. 8.5. This system is used to correlate the response parameters with soil humidity. Sampling rate for this sensor is 15 s.

The monitoring system also acquires information from a meteorological station maintained by the Department of Geophysics at the University of Chile. This station is installed on the roof of the building of the Department of Civil Engineering 40 m distant from the central tower. Every 15 min, the station collects data from temperature, precipitation, and wind speed, among others.

8.2.1.2 Network Workflow

The structural health monitoring system stores all data in a computer that also controls the acquisition system. The computer and acquisition system are located in the first basement of the structure. The computer stores and post processes the data using two system identification techniques to determine modal parameters: peak-picking and stochastic subspace identification (SSI) methods. The results are synchronized with the Civil Engineering Department server and published on Internet (www.ingcivil.uchile.cl/shm). Figure 8.6 shows the network and processing workflow used to obtain and display selected results.

To obtain the modal parameters from the time series, the system is configured to obtain continuous records packaged every 15 min. Frequency and damping ratio are updated each 15 min on the web site.

8.2.2 System Identification Technique

The stochastic subspace identification (SSI) technique developed by Van Overschee and De Moor (1996) is used to estimate modal frequency, damping, and operational shapes. This technique uses the stochastic state space model, described by Eq. (8.1), to identify modal parameters from output only response signals:

$$\begin{aligned} \{x_{k+1}\} &= [A] \cdot \{x_k\} + \{w_k\} \\ \{y_k\} &= [C] \cdot \{x_k\} + \{v_k\} \end{aligned} \tag{8.1}$$

Equation (8.1) constitutes the basis for time–domain modal identification through ambient vibration measurements. There are several techniques and algorithms to obtain modal parameters from stochastic subspace model. The mathematical background for many of such techniques is similar, differing importantly on implementation aspects. The algorithms identify the state–space matrices ($[A]$,$[C]$) based on the measurements by using robust numerical techniques, such as QR factorization, singular value decomposition (SVD), and least squares.

Once the mathematical description of the structure is found, modal parameters such as frequency, ω_i, damping ratio, ξ_i, and operational mode shapes, $[\phi]$, are determined from the eigenvalues of matrix A μ as follows:

$$\lambda_i = \frac{\ln(\mu_i)}{\Delta t} \qquad \omega_i = |\lambda_i| = \sqrt{\lambda_i \cdot \lambda_i^*} \qquad \xi_i = \frac{real(\lambda_i)}{|\lambda_i|} \qquad [\phi] = [C] \cdot [\Psi] \quad (8.2)$$

To validate results, the power spectrum density (PSD) method complemented with window correction method to obtain damping ratios is used.

The building earthquake response records have been processed with different identification techniques: modal identification (Beck 1978), modal MIMO (Mau and Li 1991, 1997), and MOESP, (Verhaegen 1994); detail of the process in the mentioned references and for the specific building can be found in Carreño and Boroschek 2010, 2011; Boroschek and Carreño 2011.

8.2.3 Results of Remote-Continuous Monitoring

8.2.3.1 Ambient Vibration, Initial Modal Parameters

Due to the continuous nature of the monitoring system, there are nearly 2 years of vibration data to statistically characterize and identify the modal parameters from ambient vibrations. Several different studies with the data have been performed including variations range for different temperature, humidity, rain, and wind conditions. Important results could be obtained from the large data set. As an example, Fig. 8.7 shows the effects on the first modal frequency and damping ratio due to temperature variations. These parameters are used as reference (signature) to identify and qualify the variations on the structure modal characteristics.

This kind of analysis is useful to recognize the nonlinear behavior due to ambient parameters and to develop parametric models of the modal properties as a function of the ambient and amplitude response characteristics. The first four mean frequency values, corresponding damping ratios, and modal shapes before the earthquake are shown in Tables 8.1 and 8.2. Mean values are used due to the dependency of the parameter with weather conditions.

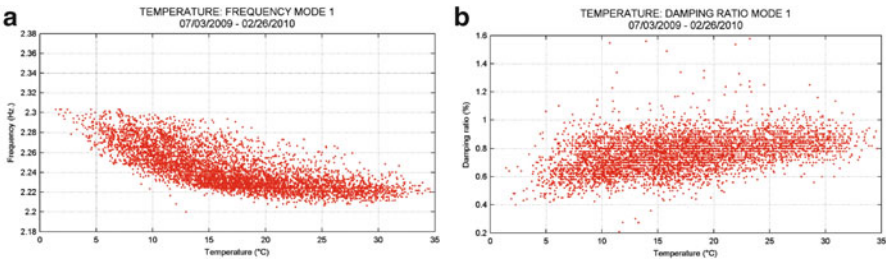

Fig. 8.7 (**a**) Temperature effects on frequency variations, mode 1. (**b**) Temperature effects on damping ratio, mode 1. Samples were taken between July 3, 2009, and February 26, 2010

Table 8.1 Frequency values obtained by PSD and SSI methods using remote SHM network

Mode	PSD f (Hz)	SSI f (Hz)	Difference (%)
1	2.23	2.23	0.00
2	2.63	2.64	0.38
3	2.99	2.99	0.00
4	6.33	6.32	0.16

Table 8.2 Damping ratio values obtained by PSD and SSI methods using remote SHM network

Mode	PSD ξ (%)	SSI ξ (%)	Difference (% of ξ SSI)
1	1.1	0.7	57.1
2	1.3	0.8	62.5
3	1.1	0.8	37.5
4	1.2	1.3	7.7

Additionally reasonably close correlations are obtained between the PSD and SSI methods, except for the damping ratio. As known, damping ratio is strongly dependent with vibration amplitude and observation window type and length.

Modal shapes are also identified with both methods. They show an acceptable correlation when compared using the modal assurance criteria (MAC) value, which is defined as follows:

$$MAC\left(\{\Psi_i\},\{\Psi_j\}\right) = \frac{\left|\{\Psi_i\}^T \cdot \{\Psi_j\}\right|^2}{\left(\{\Psi_i\}^T \cdot \{\Psi_i\}\right) \cdot \left(\{\Psi_j\}^T \cdot \{\Psi_j\}\right)} \tag{8.3}$$

where $\{\Psi_i\}$ and $\{\Psi_j\}$ are the compared modal shapes. Figure 8.8 shows the values of MAC parameter between PSD and SSI modal.

8.2.3.2 SHM Web Page Display: Correlation with Soil and Ambient Parameters

The web site designed for this building stores and publishes each selected results every 15 min on the web, and it can be accessed from any computer. The web site

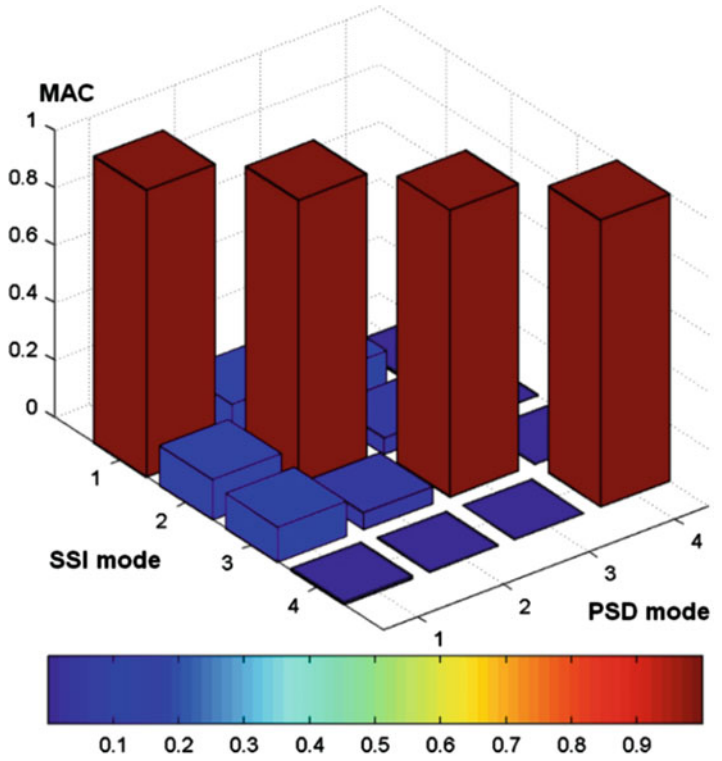

Fig. 8.8 MAC parameter between PSD and SSI modal shapes

main page shows three graphics as a function of time: The first are the modal parameters showing the frequency and damping variations. The second shows soil humidity at three different positions, and the third shows ambient parameters, Fig. 8.9. The data can be zoomed easily by the user (Yañez 2009).

8.2.4 Building Response During the Earthquake

The local strong motion network recorded several earthquakes as well as the main great event of February 27, 2010, and all the aftershocks (more than 30) Fig. 8.10. The maximum acceleration recorded at ground level during the main event was 0.16 g and the maximum structural acceleration 0.45 g. The building suffered light structural damage characterized by cracking of some structural walls and light partition damage.

The analysis of the ambient vibration-derived modal parameters before and after the main event shows a permanent change. The results indicate that there was an average increment of 14% on the first natural periods, Table 8.3. Derived damping

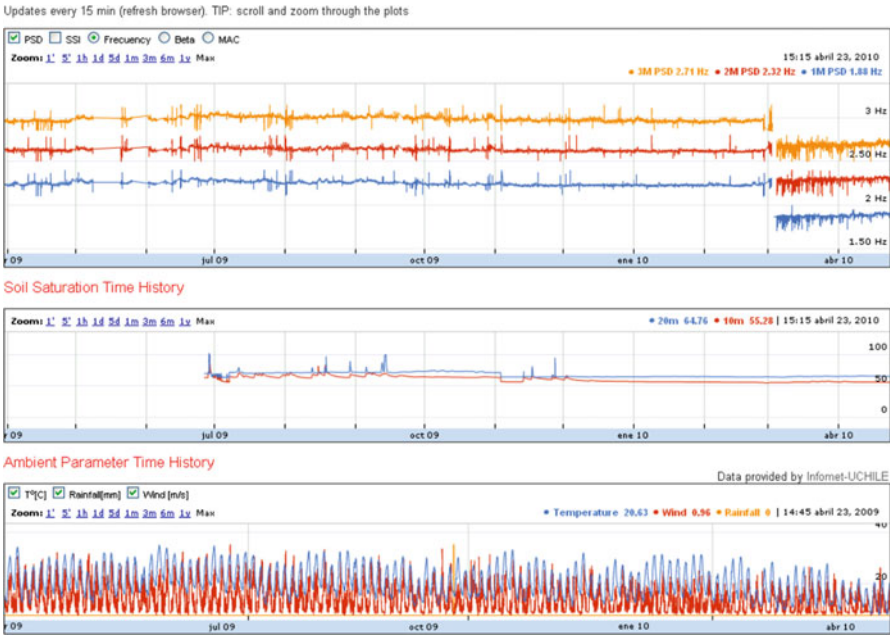

Fig. 8.9 SHM web page www.ingcivil.uchile.cl/shm

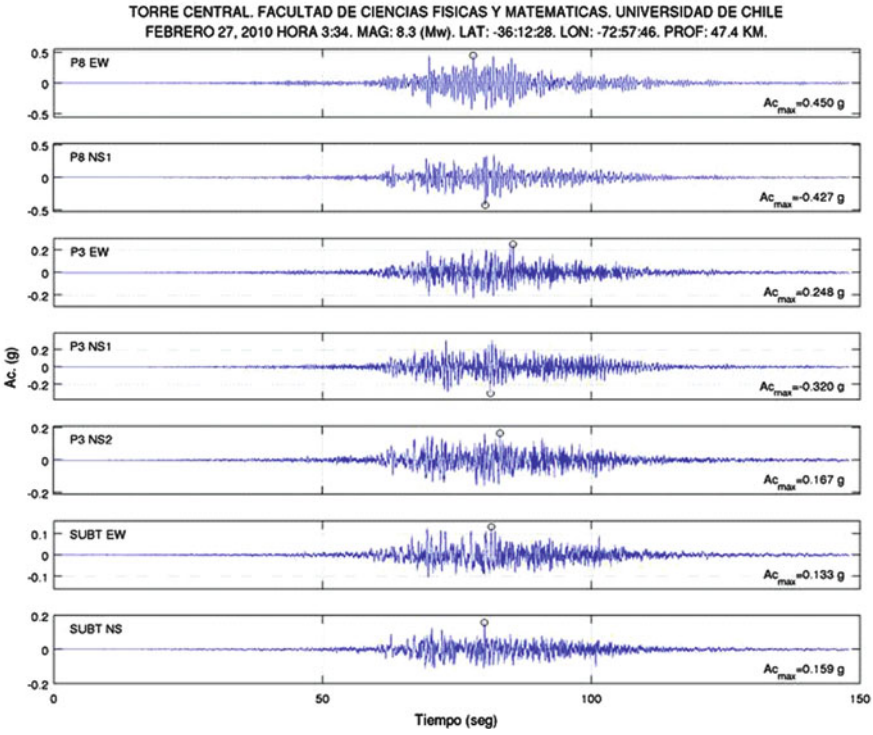

Fig. 8.10 Strong motion records of Torre Central Building

Table 8.3 Modal parameters before and after the earthquake derived from ambient vibrations

	Before		After		Difference (%)	
Mode	Period (s)	Damp (%)	Period (s)	Damp (%)	Period	Damp
1	0.45	0.7	0.53	0.7	18.6	0.0
2	0.38	0.7	0.44	0.7	14.0	0.0
3	0.34	0.7	0.37	0.8	10.9	14.3
4	0.16	1.2	0.18	0.9	15.5	25.0
5	0.13	1.5	0.15	1.3	12.1	13.3
6	0.13	0.9	0.14	1.0	12.4	11.1

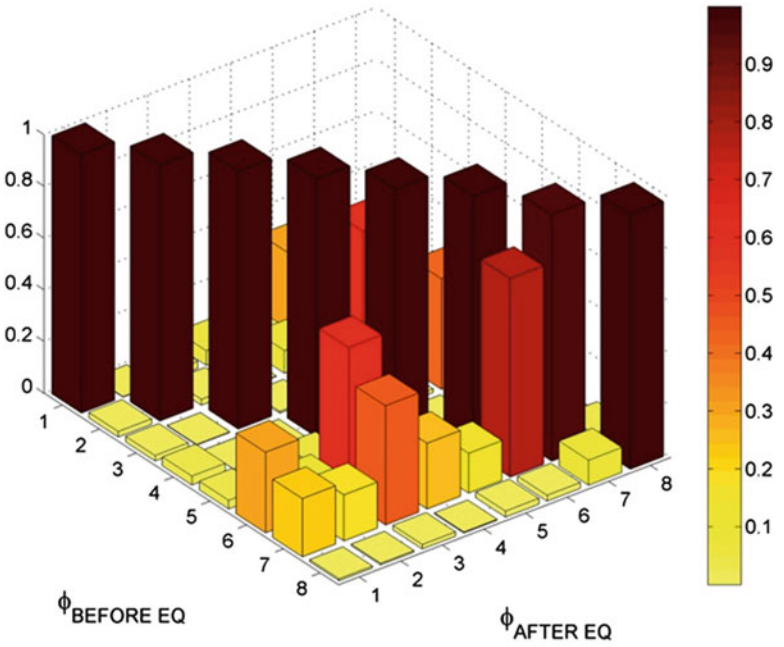

Fig. 8.11 MAC value for ambient vibration-derived modes before and after the main earthquake

values present a large dispersion. Mode shapes from pre- and post-earthquake identification process present minimum differences as can be seen from the excellent correlation between similar frequencies as observed from the MAC values presented in Fig. 8.11.

We have performed a sliding window identification analysis on the response acceleration records. Window size is 4 s. This procedure allows for the observation of the average modal properties in each window, and it is an indication of the variation of these parameters with the intensity of motion and the damage occurrence in the structure. In Fig. 8.12, we present the variation of the first four natural periods as a function of time. In the same graph but with gray scale,

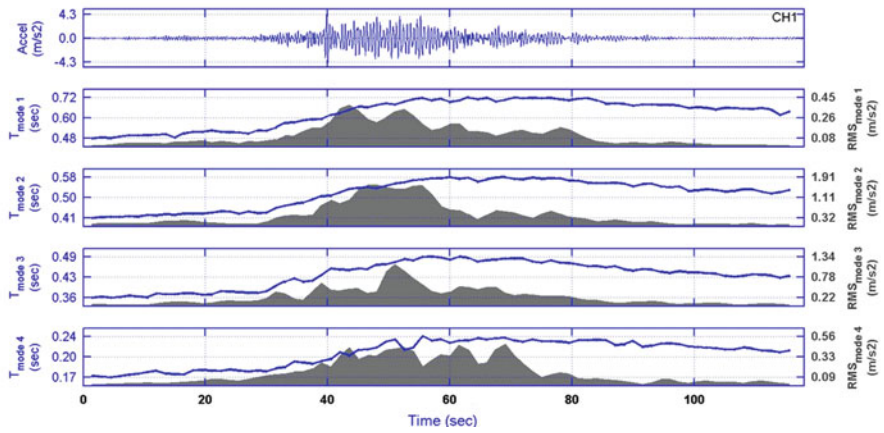

Fig. 8.12 Torre Central: natural period evolution

we present an indication of the intensity of motion of the respective mode. This intensity is captured by the root mean square (RMS) acceleration of the response of the whole building filtered around the period of interest. From these figures, we could conclude that during the strong response phase, the periods increased by as much as 40% from its initial value, recovering most of this change by the end of the records and approaching the post-earthquake ambient vibration period.

In Fig. 8.12, we observed that most of the period's change occurred after 30 s from the start of the records and is maintained during most of the strong motion phase closed to seconds at 100. This information as well as the information derived from the statistical analysis of ambient vibration-derived properties and the ambient vibration identification just before and after the earthquake, a merely maximum 15-min difference between all analyses done, gave a clear indication that the modal parameters have been permanently modified during the earthquake. The abrupt change in reported parameter can be seen on the web output in Fig. 8.9.

As a confirmation of this capability, the value for the first three modes as a function of modal response amplitude earthquake records including those events before and after the strong shaking has been plotted in Fig. 8.13. We have used different colors to represent the pre- and post-earthquake data. This figure clearly shows the increase in fundamental periods due to the increase in modal amplitude intensity, but in addition, we clearly see the strong jump of period values due to the earthquake damage. For example, the first mode period during ambient vibration before the earthquake is close to 0.45 s, and it increases for the data we have without damage until 0.48 s. During the earthquake, light damage occurred changing the low amplitude period from 0.45 to 0.55 s. During post-earthquake seismic events, the new values range from 0.55 to 0.65 s.

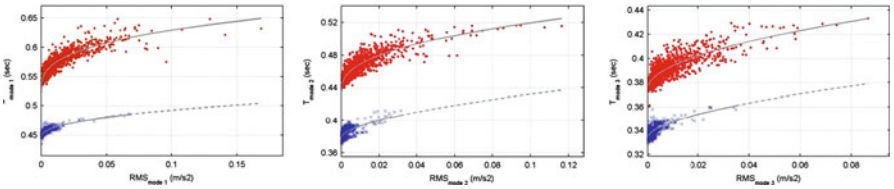

Fig. 8.13 Torre central period change due to response intensity and damage

8.3 Chilean Construction Chamber Building

This building has 22 stories and 4 underground levels. It was constructed at the end of 1980s for office use. Its structural system is based on a thick reinforce concrete wall at the central core and some light perimeter frames and walls, Fig. 8.14. The floor area is 960 m^2, and the total building area is 28,600 m^2. The building is regular in plan and elevation. The total building height is 85.5 m, 72.5 m of which is above ground. Typical floor height is 3.3 m. The building is located in Santiago, Chile, on gravelly soil.

The structural system corresponds to a dual frame wall system with predominance of the structural walls. Gravitational loads are supported by the frames and the walls. Lateral forces are resisted by the walls. The main core wall and central columns are supported on a single 1.5-m thick foundation slab. Underground perimeter walls are 30 cm thick. The main structural wall has an H shape with stiffened flanges. The thickness of this main wall changes four times in height. The ratio of wall area to floor area for the underground stories is 6.3%, and for the above ground stories 4%. Despite this large value, the plan areas are free for office use because of the arrangement of the structural systems. Above ground floor slabs are 15-cm thick.

8.3.1 Instrumentation and Sensor Layout

This is the first permanently instrumented building in Chile. Initially the instrumentation consisted in tree independent triaxial analog accelerograph located at the ground and at the middle and top levels. This system never recorded the earthquake so it was replaced by a digital network in 1995, with the help of the Chilean Science and Technology Council, CONICYT. The new network that has been in place for more than 16 years consists of 12 uniaxial force balance accelerometers connected to a central recording unit, Fig. 8.15. The sensors register the analog acceleration with a dynamic range of 135 dB between 0.01 and 50 Hz and 145 dB between 0.01 and 20 Hz. The analog signal is converted in to a digital record in the central recording unit with a-19 bit resolution. This bandwidth and dynamic range allows the recording of ambient and earthquake records with the same system. Three sensors are located horizontally on the 12th and 19th floors, two sensors are at

Fig. 8.14 General view of the Chilean Construction Chamber Building

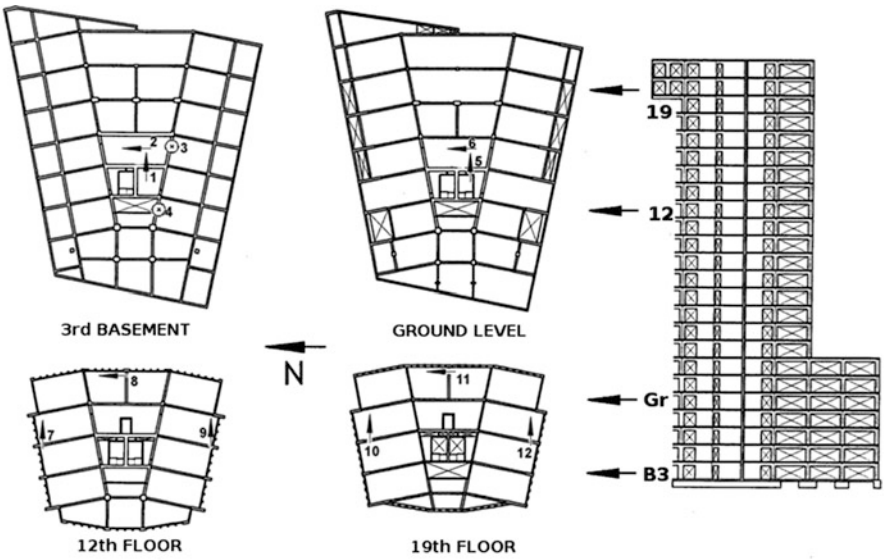

Fig. 8.15 Sensor location

Fig. 8.16 Structural and nonstructural damage (Photo Bartolomé-Caroca)

ground level, and two horizontal and two vertical sensors at the fourth underground level. This sensor distribution allows for the monitoring of the spatial motion of the structure, the identification of the modal properties, and the partial capturing of its linear and nonlinear response characteristics.

This network has registered more than 60 seismic events and many months of continuous ambient vibrations. The vibrations have been processed, and the basic modal properties of the structure identified together with the response properties.

8.3.2 Earthquake Response

During the 2010 earthquake, the building presented light structural and nonstructural damage. The damage was concentrated mainly in the perimeter concrete wall and frames and in some nonstructural partitions and ceilings, Fig. 8.16.

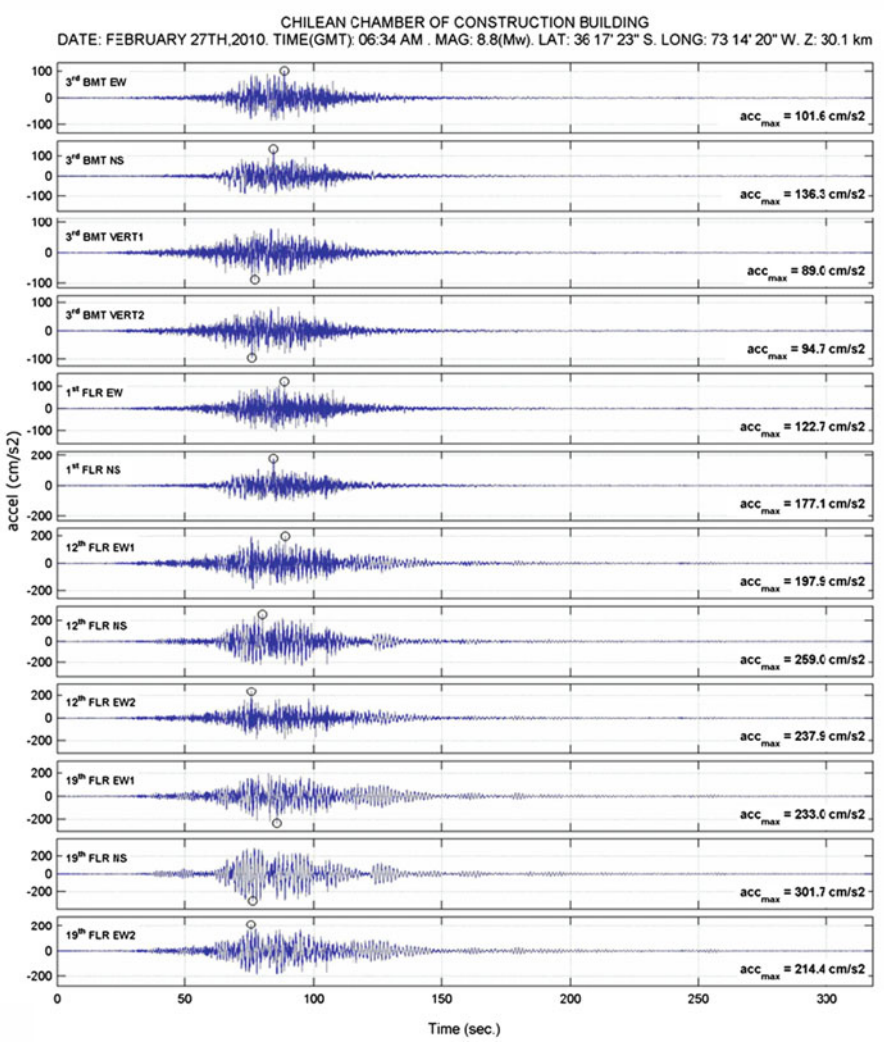

Fig. 8.17 Acceleration records from the Feb 27, 2010 event

The strong motion recording system works perfectly allowing the recording of the main event a several aftershocks and new earthquake events. Figure 8.17 shows the acceleration time series obtained in the building. The maximum acceleration at ground level was 0.17 and 0.097 for the horizontal and vertical direction, respectively. On the above ground structure, the maximum recorded acceleration was 0.31 g. The record shows the long duration characteristics of this earthquake presenting a strong response for more than 50 s and perceptible vibration for more than 2 min. The records also show the effect of the two high energy releases that characterized this event. The maximum response in the different locations

Table 8.4 Period and damping before and after the 2010 earthquake

	Before		After			
Mode	Period (s)	Damp (ξ) (%)	Period (s)	Damp(ξ) (%)	Diff period (%)	Diff damp (%)
1	0.99	0.6	1.19	0.6	20.2	0.0
2	0.97	0.7	1.16	0.6	19.8	14.3
3	0.65	0.6	0.82	0.8	26.2	33.3
4	0.29	1.1	0.34	1.1	18.6	0.0
5	0.29	1.2	0.35	1.1	20.3	8.3
7	0.22	1.1	0.27	1.1	25.9	0.0
				Average	**21.8**	**9.3**

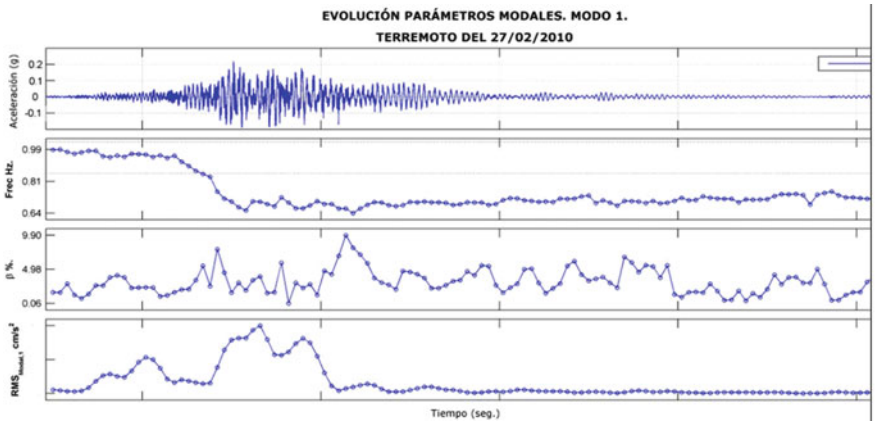

Fig. 8.18 Evolution of first mode frequency, damping, and RMS modal intensity

depends strongly on the input and building characteristics. In this particular case, the building had their maximum acceleration response associated with the first asperity close to the epicentral area and not to the closes asperity located close to Pichilemu. The records also show the beating phenomena associated with the close modes that are present in this building, see, for example, the response of the 19th floor between 100 and 150 s.

First, we identify the modal properties from pre- and post-earthquake ambient vibrations in order to evaluate possible permanent change on these properties. Table 8.4 shows the result of the identification process for the first seven predominant periods and damping. From this table, it is possible to conclude that the observable damage on the structure had an effect mainly on the natural periods. The typical change in periods was around 22%. The change in damping was minimal and non-conclusive by itself.

In a similar way as indicated in the previous building, we have performed a system identification using nonoverlapping sliding windows. Figures 8.18 and 8.19 present the frequency change as a function of time for a window of 4-s duration.

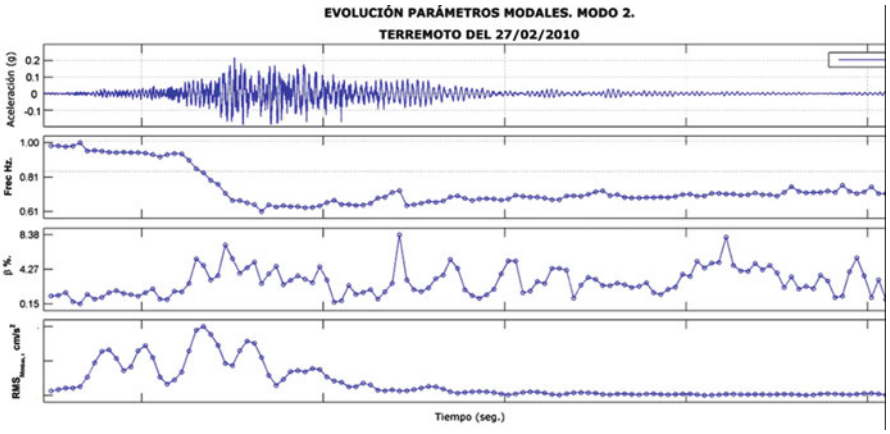

Fig. 8.19 Evolution of second mode frequency, damping, and RMS modal intensity

Table 8.5 Natural frequency during the earthquake

				Relative difference (%)	
Mode	Start (Hz)	Minimum (Hz)	End (Hz)	Minimum	Fin
1	0.99	0.64	0.79	35.2	20.1
2	0.98	0.61	0.74	37.8	24.8
4	3.72	2.44	3.02	34.6	19.0
5	3.36	2.31	2.65	31.1	21.2
			Average	34.7	21.3

On top of each figure, we present one characteristic acceleration record, below the variation of the natural frequency, the variation of damping, and the RMS value of the modal response. From the frequency variation on both figures, we can conclude that the main change on natural frequency started with a ground acceleration amplitude higher than 0.08 g after that, no permanent change in natural frequency occurred. When the amplitude of the response diminished, the natural frequency increased to a value close to the post-earthquake ambient vibration level.

The initial, minimum, and final values for the first five frequency modes are presented in Table 8.5. From these values, it is possible to detect the strong variations that suffer these parameters during the different motion intensities reaching values that differed in nearly 40%. This is an important result considering that only light damage was present in the building. An important consideration is that these variations are dependent on amplitude of the response, so they could disappear if no damage is present.

As mentioned before, this period sensitivity to intensity of response has been observed before on other buildings. We have studied this variation using 60 different intensity records for this building. Figure 8.20 presents the variation for the first two modal frequencies and damping as a function of the RMS value of the modal response and for a sliding window of 4-s duration. The February 27, 2010, earthquake has been outlined using different colors and separating different critical

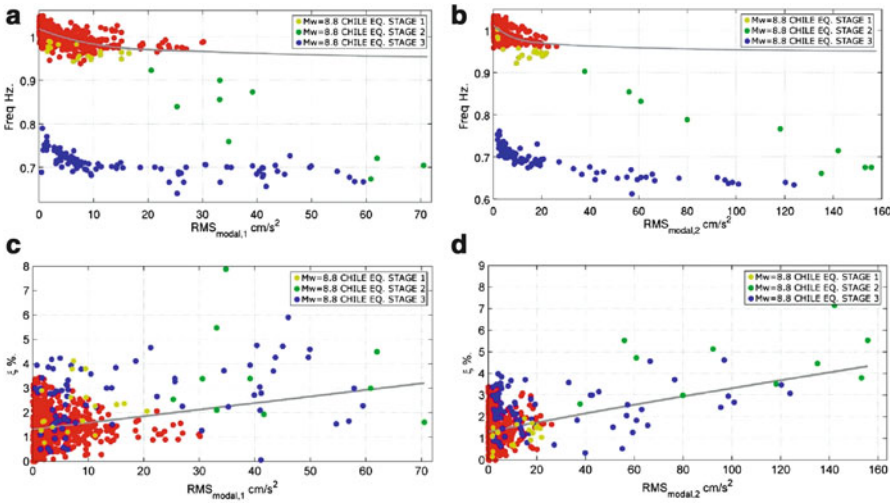

Fig. 8.20 Change in frequency and damping as a function of modal RMS amplitude

section of the record. The red dots are the identified properties before the 2010 main event. The yellow dots correspond to the start of the 2010 main event, the green dots correspond to the strong phase part of the records, and the blue ones to the final low amplitude part of the record. From this figures and color scheme, it is clearly seen the abrupt change on the value of frequency and damping due to earthquake damage. For example, the natural frequency for low amplitude motions changes from 1.05 to 0.8 Hz. Damping does not show this clear change. It is also clear from these figures that the frequency in its undamaged or damage state is reduced when the RMS value increases and that damping increases with RMS values. The change in frequency is nearly 35%, and the change in damping for the same conditions can be as high as 500%.

8.4 Conclusion

The great 2010 Chilean earthquake due to its large magnitude affected an extensive and disperses stock of structures. Several critical structures and buildings suffered different degrees of damage. There was a desperate call for evaluation and a severe scarcity of human resources. The pressure to the engineering community to give conclusive opinions to the society on the safety of its structure lasted for months. It is possible to envision that this stressful situation could have been diminished if a large stock of structure has been instrumented with a comprehensive monitoring network and an effective structural health monitoring system had been in place.

We have described the characteristics of two building SHM systems located in Chile. They were able to record and detect a permanent change in dynamic properties of the system, one of which reported in less than 15 min after the event

in a web-based system. We envision this system as an important advance in earthquake engineering and community response to large earthquakes.

There are areas of needed research and advance, for example, the understanding of the nonlinearities of the system response to environmental and used conditions and the knowledge of damage magnitude and its location. In addition, to make this technology widespread, we need to reduce the cost of instrumentation, installation, maintenance, and robust communications.

Acknowledgments The Civil Engineering Department of the University of Chile and the Chilean Council for Research and Technology, CONICYT, Fondecyt Project # 1070319 supported this research paper. Engineer Pedro Soto for their collaboration and support in the development of this study.

References

Assimaki D, Ledezma C, Montalva GA, Tassara A, Mylonakis G, Boroschek R (2012) Site effects and damage patterns. Earthquake Spectra, June 2012, 28(S1):S55–S74

Beck JL (1978) Determining models of structures from earthquake records. Report EERL 78–01, Caltech, Pasadena, California

Boroschek R, Carreño R (2011) Period variations in a shear wall building due to earthquake shaking. 5th international conference on Structural Health Monitoring of Intelligent Infrastructure (SHMII-5), Cancun, México, 11–15, December 2011

Boroschek R, Núñez T, Yáñez T (2010) Development of a real time internet based monitoring system in a nine story, shear wall building. 14 European conference in earthquake engineering, Ohrid Macedonia, Paper 1215, pp 7

Boroschek R, Contreras V, Youp D, Stewart J (2012) Strong ground motion attributes of the 2010 Mw 8.8 Maule Chile earthquake. Earthquake Spectra. Accepted for publication

Carreño R, Boroschek R (2010) Variation of dynamic properties of the Chilean chamber of construction building: Seismic case. X Jornadas Chilenas de Sismología e Ingeniería Antisísmica, Santiago, May 2010, Paper H3 (In Spanish)

Carreño R, Boroschek R, (2011) Modal parameter variations due to earthquakes of different intensities. International Modal Analysis Conference, IMAC XXIX, Jacksonville, Florida, 31 January–3 February 2011, paper 228, pp 13

Delouis B, Nocquet J-M, Vallée M (2010) Slip distribution of the february 27, 2010 Mw = 8.8 Maule earthquake, central Chile, from static and high-rate GPS, InSAR, and broadband teleseismic data. Geophy Res Ltrs 37:L17305

Mau ST, Li Y (1991) A case study of MIMO system identification applied to building seismic records. Earthquake Eng Struct Dyn 20:1045–1064

Mau ST, Li Y (1997) Learning from recorded earthquake motion of buildings. J Struct Eng 123:62–69

Van Overschee P, De Moor B (1996) Subspace identification for linear systems: theory-implementation-applications. Kluwer Academic Publishers, Dordrecht

Verhaegen M (1994) Identification of the deterministic part of MIMO state space models. Automatica 30:61–74

Yañez T (2009) Implementation of continuous monitoring network, dynamic parameters identification system of a shear-wall building. Civil Engineering Thesis. University of Chile (In Spanish)